JOURNAL OF
EMERGING INVESTIGATORS

Article

Development of selective RAC1/KLRN inhibitors

J. Kubrat Neczaj-Hruzewicz[1], Natalie Dixon-Hernandez[2], Thomas Grimes[3], Mia Callens[3], Paul E. Brennan[3]

[1] St. Clare's School, Oxford, United Kingdom

[2] Cherwell School, Oxford, United Kingdom

[3] Centre for Medicines Discovery, Nuffield Department of Medicine, Oxford University, United Kingdom

SUMMARY

Kalirin, named after the multidextrous Hindu goddess Kali for its ability to interact with multiple proteins, is a GEF (guanine nucleotide exchange factor) for the GTPase (enzyme hydrolyzing guanosine triphosphate to guanosine diphosphate) RAC1 that has been found to correlate with schizophrenia and Alzheimer's Disease. Restoration of brain function through synaptic plasticity, the ability of neurons to modify the strength of their connections, offers much promise in the struggle against neurodegeneration. Kalirin contributes to synaptic plasticity through regulation of dendritic spine morphogenesis and actin cytoskeleton remodeling, both of which facilitate formation of new synapses. Therefore, developing kalirin selective inhibitors may give valuable insight into its function and possible effects on human health. We developed two novel compounds based on previous research on kalirin inhibitors. We partially confirmed the hypothesis that the in silico model's accuracy in scoring novel chemical entities is a predictor of biological activity against the RAC1/kalirin target. We designed two novel compounds, we docked them in a computer model of the active site, we synthesized, and then tested their biological activity in an assay and compared against the model's predictive score for binding to the active site. Compounds 3 and 4 had limited activity against RAC1/kalirin in a nucleotide exchange assay but gave useful insight into future structure-based design and development of kalirin selective inhibitors. Hence, we propose further structural modifications for the synthesis of more biologically potent and selective RAC1/kalirin inhibitors.

INTRODUCTION

Prior work on schizophrenia and Alzheimer's disease in postmortem brains and knockout studies in mice has established a correlation between these diseases and the protein kalirin, a guanine nucleotide exchange factor (GEF) for the enzyme hydrolyzing guanosine triphosphate to guanosine diphosphate (GTPase) RAC1 (1). Schizophrenia is a chronic and severe mental disorder that affects cognition, emotions and behavior. Symptoms include hallucinations, delusions, and diminished emotions, as well as thought, speech, and movement disorders. Cognitive symptoms are manifested through difficulties with attention, memory, and executive functons such as planning and organizing.

Presently, there are no effective established therapeutic interventions for the cognitive deficits observed in individuals diagnosed with schizophrenia (2). Current treatments for schizophrenia primarily focus on managing symptoms through medication and therapy. Common schizophrenia medications include antipsychotics that reduce severity of hallucinations and delusions. Apart from significant side effects such as movement disorders, weight gain and diabetes, a fundamental limitation of these medications is that they manage symptoms rather than targeting the underlying disease, leaving subjects uncured (2). Promising avenues of research to improve schizophrenia treatment include managing neuroinflammation and regulating synaptic function and plasticity. The first approach investigates the role of neuroinflammation in schizophrenia with the goal of developing targeted anti-inflammatory therapies to restore neuronal function. In the second approach, understanding how kalirin and RAC1, a GTPase that binds to the nucleotide guanosine triphosphate (GTP) and hydrolyzes it to guanosine diphosphate (GDP) as shown in **Figure 1**, regulate synaptic function and plasticity can reveal new targets for therapeutic intervention. Since schizophrenia is associated with synaptic abnormalities, modulating the activity of these proteins might help restore normal synaptic function.

Thus, augmentation of synaptic plasticity presents a novel approach to ameliorate cognitive functions in patients with schizophrenia (3–8). Kalirin, a protein encoded by the KALRN gene, is instrumental in the formation and stabilization of dendritic spines (9). These spines are small protrusions that receive inputs from an axon at the synapse. Dendritic spines impact synaptic strength and help in transmitting electrical signals to the neuron. Kalirin plays a crucial role in the development and maintenance of neuronal architecture, which is often disrupted in schizophrenia. Alterations in kalirin expression have been implicated in psychiatric disorders, including schizophrenia.(9-10) Consequently, kalirin has emerged as a potential target for therapeutic strategies aimed at enhancing cognitive performance in schizophrenia (9). However, it is not clear which specific kalirin isoforms that would be most efficacious as therapeutic targets. There are 5 major isoforms, resulting from alternative splicing. They differ in structure and function

RAC1 is involved in actin cytoskeleton organization, gene transcription, and cell proliferation. Dysregulation of RAC1 signaling has been linked to cognitive deficits and synaptic dysfunctions observed in schizophrenia. Mutations in both kalirin and RAC1 have been implicated in schizophrenia

https://doi.org/10.59720/24-033

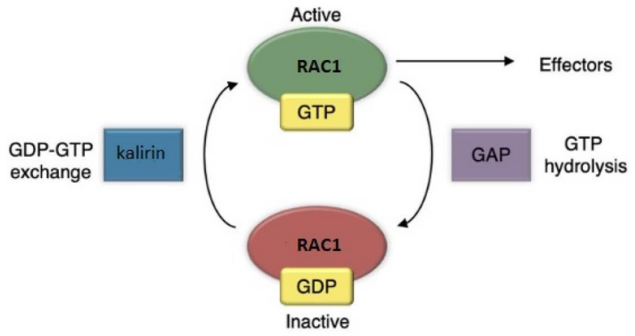

Figure 1: RAC1/kalirin schematic. Diagram showing how GEFs such as kalirin facilitate nucleotide exchange for GTPases such as RAC1. GTPase activating protein (GAP) in turn downregulates RAC1.

(10,11).

Alterations in the actin cytoskeleton are fundamental to the genesis, stabilization, and plasticity of synaptic structures (12). These dynamics of actin are, in turn, modulated by the RHO family of small GTPases (13). The RHO GTPases, a subset of the RAS (from rat sarcoma virus) superfamily, encompass approximately 20 small G-proteins. They play a critical role in an array of both physiological and pathological processes. Functioning as molecular switches, RHO GTPases oscillate between an active GTP-bound state and an inactive guanosine diphosphate (GDP)-bound state (14). This oscillation enables them to respond to diverse external stimuli and regulate broad cellular functions, including morphology, proliferation, and gene expression (14).

In neuronal contexts, RHO GTPases are pivotal in translating extracellular cues into cytoskeletal reconfigurations, which are essential for the formation and maintenance of dendritic spines. The transition between their active and inactive states is regulated by GEFs such as kalirin. These factors promote the conversion from the GDP-bound form to the GTP-bound form, thereby augmenting the activity of the GTPase.

RHO GTPases are classified into several subfamilies, namely RHO, RAC, Cdc42, RHOD, RND, and RHOH, based on sequence homology (14). The interplay between RHO GTPase activity and actin cytoskeleton rearrangement is complex, attributable to the unique yet complementary functions of different family members. RAC1, which belongs to the RAC subfamily, stimulates actin polymerization. Via this mechanism, RAC1 not only promotes the formation of dendritic spines but also plays a crucial role in facilitating processes related to learning and memory (15).

GEFs like kalirin facilitate the exchange of GDP for GTP by inducing conformational changes in small GTPases that decrease their affinity for GDP and increase their affinity for GTP (**Figure 1**). Specifically, kalirin binds to the inactive, GDP-bound form of RAC1 and induces a conformational change leading to GDP release and rapid binding of GTP, which is present at higher concentrations in the cell. This GDP to GTP exchange is a critical step in the activation of small GTPases and their subsequent signaling. GTP-bound RAC1 interacts with downstream proteins to enact various cellular responses, such as changes in the actin cytoskeleton, cell migration, and growth.

The KALRN gene is responsible for encoding a variety of kalirin protein isoforms using alternative splicing and promoters, which affect the point where transcription is initiated resulting in different N-terminal sequences (16–19). Rare variants in the KALRN gene have been identified that are more prevalent in individuals with schizophrenia than in control groups (20, 21). These genetic findings are further corroborated by family-based studies (22). Knocking out the KALRN gene would remove expression of all isoform activity nonselectively. Total lack of the gene leads to lack of expression of all isoforms that differ by alternative splicing but all equally require expression. Only through selective inhibition of indi-

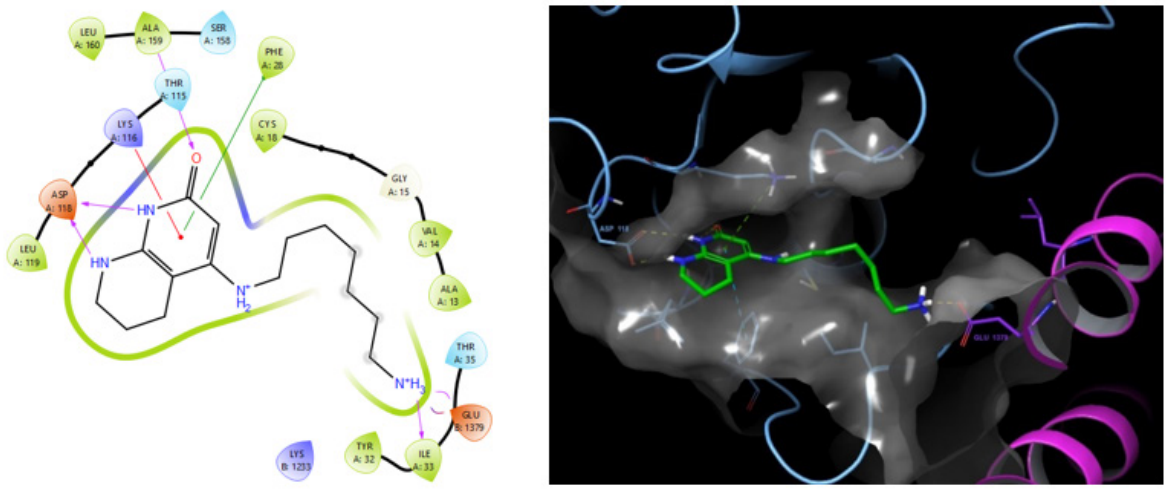

Figure 2: Interaction diagram (left) and docking pose (right) of compound 2. The structure of compound 2 are shown in its modelled position within the active sites of RAC1/kalirin. Docking was performed using the RAC1/GDP/kalirin X-ray crystal structure (PDB ID 5o33). Kalirin is colored in pink, while RAC1 is colored in blue. The key interactions of compound 2 with RAC1 are with Asp118, Lys116 and Thr115. Compound 2 also interacted with kalirin at Glu1379. In the interaction diagram on the left, basic amino acids are shown in purple, acidic in red, hydrophobic in green, and H-bond donors with hydroxyl side chain in blue.

https://doi.org/10.59720/24-033

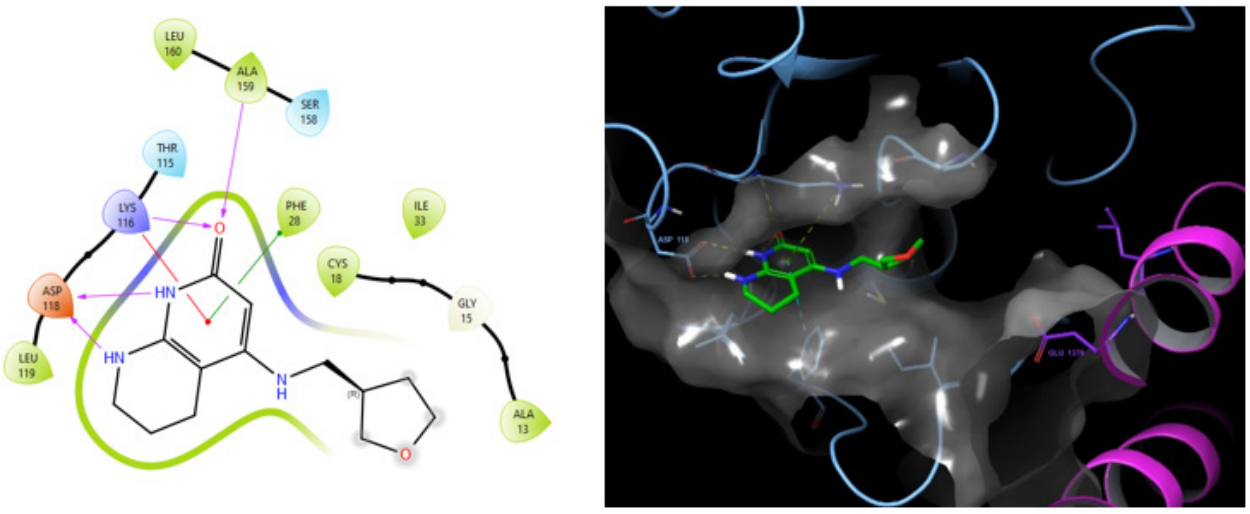

Figure 3: Interaction diagram (left) and docking pose (right) of compound 4. The structure of the designed compound is shown in its expected position within the active site of kalirin/RAC1. Docking was done using the same X-ray crystal structure as before (PDB ID 5o33). Kalirin is colored in pink, while RAC1 is colored in blue. The key interactions of compound 4 with RAC1 are with Asp118 and Lys116; compound 4 doesn't have any interactions with kalirin. In the interaction diagram on the left, the basic amino acids are shown in purple, acidic in red, hydrophobic in green, and H-bond donors with hydroxyl side chain in blue.

vidual kalirin isoforms can their effect on dendritic formation be selectively modulated and studied.

Therefore, selective kalirin inhibitors, which give one more control over biological activity than indiscriminately knocking out the gene function, may provide a tool in elucidating the impact of synaptic plasticity on brain function. Structure-based design relies on computer simulations of docking novel chemical structures in a model of the active site prior to synthesis in order to accelerate and improve effectiveness of the design-synthesize-test cycle. Compound **1** (the core) only binds to RAC1, and the purpose of this investigation is to synthesize a compound that binds to the pocket in RAC1, but which extends to kalirin, and increases selectivity for the GEF in this way. Potent binders could be later tested for selectivity against various kalirin isoforms as tools to modulate gene product activity.

To that end, selective inhibitors of kalirin/RAC1 are needed in order to elucidate the details of disease mechanism. Our hypothesis, that we further explore in this paper, is that the *in silico* model's accuracy in scoring novel compounds would predict biological activity against the kalirin/RAC1 target.

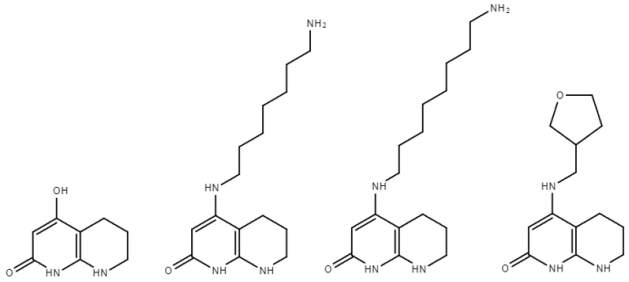

Figure 4: Structures of compound 1–4 in order. Compound 1 is a previously synthesized GTP-competitive RAC1/kalirin inhibitor with robust biological activity. Compound 2 is a hypothetical model of a selective RAC1-kalirin inhibitor. Compounds 3 and 4 were synthesized and tested in this study.

Therefore, we set out to design, synthesize, and test several potential inhibitors based on the predictions of this model.

RESULTS

The purpose of this investigation was to develop compounds that bind to RAC1/kalirin based on previously synthesized and tested molecules that inhibit kalirin dependent RAC1 nucleotide exchange. The goal was to also increase potency and selectivity for kalirin over other similar Rho GEFs. The investigation consisted of three steps: docking/design of molecules, chemical synthesis and biological activity assays.

Design and docking of molecules

We docked a virtual library of compounds in a simulation program and selected for expected activity based on the docking score and availability of starting materials as well as ease of synthesis **Figures 2** and **3**. To test the predictive strength of the docking model, we synthesized compound 3 – we expected it to have higher affinity for kalirin than a previously synthesized compound **1** (**Figure 4**), which showed modest inhibition of the RAC1/kalirin complex 100% inhibition at 500 μM.

The assay results did not confirm this prediction, which could imply that the docking model needs further refinement. Compound 4 was synthesized to test the hypothetical importance of the RAC1 interaction in the active site per docking model, but this hypothesis was not confirmed in a binding assay.

To synthesize kalirin selective inhibitors we started by designing and docking a virtual library of over 100 analogs of compound 1 that retained the key bidentate interaction with RAC1 Asp118. While we considered synthetic feasibility, our primary objective was to test various geometries and interactions with the target protein. Therefore, we designed the 100 analogs semi-rationally to maximize the exploration of binding site geometry and binding affinities of various functional groups. Compound 1 which was discovered

https://doi.org/10.59720/24-033

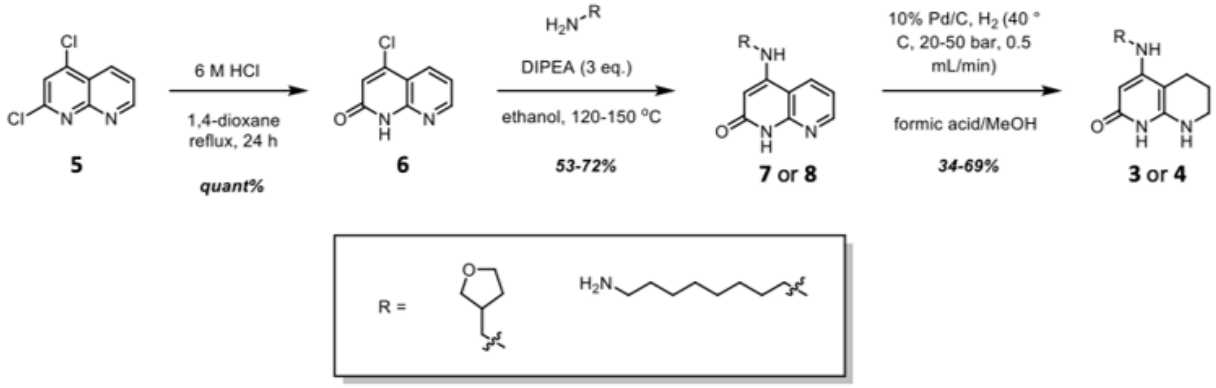

Figure 5: Synthesis of compounds 3 and 4. The chemical synthesis was done in three steps, which were analogous for both compounds. The R group used in the second step is shown in the box and differentiates compound 3 and 4. The summary of reaction conditions and the yields for each step are shown above.

via5virtual screening showed modest inhibition of the RAC1/kalirin complex achieving 100% inhibition at 500 uM.

By extending the molecule out of the RAC1 nucleotide pocket towards kalirin, we hoped to increase potency and selectivity (**Figure 2**). We designed compound 2 with a seven-carbon chain terminating in a primary amine interacting with Glu1379, a residue from kalirin (**Figure 2**). The docking score predicted that compound 2 would be more potent than compound 1. To explore structural boundaries, the eight-carbon chain compound 3 was synthesized instead which was based on the same criteria but had a slightly inferior docking score to 2, -6.34 vs -6.70. We also synthesized compound 4, which had no interactions with kalirin in the docking model but had additional lipophilic interactions between the tetrahydrofuran ring and Ala13 of RAC1, with a docking score of -6.96 (**Figure 3**). The software calculated the docking score on the basis of hydrogen bonding, electrostatic, hydrophobic and van der Waals force using Glide XP.

Synthesis of molecules

We synthesized the novel molecules in three steps, starting from commercially available 2,4-dichloro-1,8-naphthyridine (**Figure 5**). For compound 3, the yield of the first step was quantitative, the yield of the second step was 51.7% and the purity was 52%. The yield of the third step was 33.8% and the purity after HPLC (high performance liquid chromatography purification) was above 90%. The structure of the final product was confirmed by NMR (**Appendix**).

For compound 4, the yield of the first step was also quantitative, the yield of the second step was 72.5% and purity 77% and the yield of the third step was 69% and post HPLC purity was above 90%. The structure of the final product was confirmed by ^{1}H and ^{13}C NMR (**Appendix**).

Activity against RAC1/kalirin

We used a nucleotide exchange assay to measure RAC1/kalirin activity because it directly quantifies the ability of kalirin, as a GEF, to facilitate the exchange of GDP for GTP on RAC1, providing quantitative data on the rate of nucleotide exchange, and allowing precise determination of GEF activity. We tested compounds 3 and 4 along with compound 1 in a nucleotide exchange assay to evaluate their activity against RAC1/kalirin (23) (**Figure 6**). We prepared samples of varied concentrations of test compounds, with GppNHp (guanosine-5'-(β,γ-imido)triphosphate, which is a non-hydrolyzable analog of GTP) serving as positive control. After a two-hour incubation, the fluorescence signal was measured every thirty seconds for five minutes. The initial enzyme rate was calculated and normalized with respect to the GppNHp control. Temperature, pH and concentrations were controlled rigorously.

Compound 4 had an IC50 of 500 μM, the highest concentration tested, while compound 3 did not show any inhibition (**Figure 6**). Above a certain concentration, a decrease in rate of nucleotide exchange is expected which would indicate inhibition. IC50 is a 50% inhibition and IC100 is complete inhibition. These results are not necessarily unexpected as compounds 3 and 4 did not dock as well as compound 2, which we were unable to synthesize.

DISCUSSION

In this study, we wanted to investigate the inhibition of RAC1/kalirin which can eventually shed more light onto schizophrenia mechanisms. To achieve this, we began with a design/docking cycle, synthesized the design inhibitors

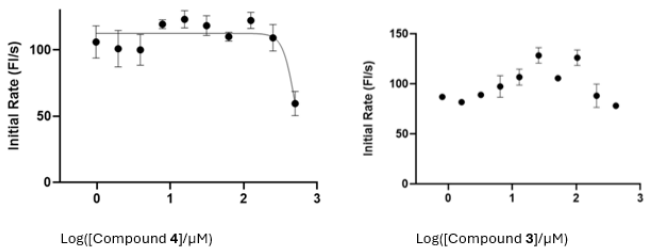

Figure 6: IC_{50} curves for compounds 3 and 4 in a nucleotide exchange assay with RAC1/kalirin. The assay results show the rate of nucleotide exchange on the y-axis as a function of a log of concentration of a compound of interest. Log 0 to log 3 in micromolar terms translates into a concentration range of 1 μM to 1000 μM. Compound 4 showed 50% inhibition at approximately 500 μM. Compound 3 showed no correlation between nucleotide exchange rate and concentration and thus no inhibition.

https://doi.org/10.59720/24-033

and conducted biological assays. Two novel compounds (3 and 4) were successfully synthesized. They had limited activity against RAC1/kalirin in a nucleotide exchange assay, but partially confirmed *in silico* hypotheses and gave useful insights into further development of kalirin-selective inhibitors. The purpose of this study was two-fold. First - to verify the predictive nature of modeling for developing potent RAC1/kalirin inhibitors using an *in silico* docking score to anticipate biological activity. Second – to yield potent RAC1/kalirin inhibitors that would themselves be useful for further study and may also provide a basis for design of additional structural analogues. Such analogues may aid in further study of the role of RAC1/kalirin in schizophrenia.

In relation to these goals, the study was partially successful. Correlation with the docking score can indeed be deduced, and good input for further structure-based design has been generated, wherein specific structural modifications should yield increased activity. However, among the molecules we synthesized, none was a potent inhibitor of RAC1/kalirin nucleotide exchange.

The nucleotide exchange assay has limitations resulting from the *in vitro* conditions used. A cellular environment contains other regulatory proteins and factors that modulate RAC1 and kalirin activity, and these added complexities may limit our ability to extrapolate our results to an in vivo system. However, these limitations do not hinder the conclusions from the nucleotide exchange assay.

Other possible assays that were considered were a GTPase Activation Assay, FRET and BRET. The GTPase Activation Assay uses a pull-down method with a GTP-bound RAC1 binding domain to selectively isolate and measure the amount of active RAC1. This assay provides information on the overall activation state of RAC1 in the presence of kalirin but is less direct in measuring the nucleotide exchange process. Foester Resonance Energy Transfer or FRET-based sensors can be designed to detect the interaction between RAC1 and GTP in live cells. These assays offer real-time monitoring of RAC1 activation and can be highly specific and sensitive. Similar to FRET, BRET uses bioluminescent proteins to study protein-protein interactions and can be used to monitor RAC1 activation in real time. However, since the experiment design was not focused on live cells, we chose the nucleotide exchange assay as the most accurate, facile and direct measure of RAC1/kalirin activity.

Our modeling suggested that a tetrahydrofuran would have a good geometric fit and a stabilizing polar interaction with the pocket. The terminal amine of compound 3 showed a positive interaction with the negatively charged Glu1379 of kalirin. The tetrahydrofuran moiety of compound 4 did not improve binding through the modeled interaction with RAC1, in comparison to compound 1. This could imply either a weakness of the docking model or lack of relevance of the RAC1 interaction. The eight-carbon long alkane chain of compound 3 was a concern in terms of perturbing interactions of Thr115 and Asp118. This carbon chain appeared too long, and the base of the molecule lost the key bidentate interaction with Asp 118; therefore, its binding affinity was expected to be moderate at best.

Availability of starting materials precluded us from synthesizing compound 2, but future work could synthesize and test this seven-carbon analogue, as it yielded a superior docking score compared to compound 3. The shorter carbon chain should improve interactions between two ends of the pocket, which was disrupted in the docking model of compound 3, potentially restoring the bidentate interaction with Asp118. Additionally, it would be interesting to move the attachment of the long carbon linker to a different position on the molecule. This may allow the compound to interact more extensively with kalirin to increase selectivity. In the future, we could also build additional functionality onto the long carbon chain and explore other interactions with the residues inside the kalirin binding pocket. Adding polar functional groups onto the long alkane chain would increase polarity and may improve solubility of the target compounds.

Selective inhibitors of individual isoforms may shed light on whether inhibiting particular kalirin variants can provide relevant data with regards to schizophrenia and Alzheimer's disease pathologies. Once higher binding affinity to kalirin can be achieved, the compounds could be screened for selectivity against other isoforms. A mid-term objective of a follow-up study would be to identify a selection of highly potent binders. These could be tested against various isoforms of kalirin and other GEFs to identify the most selective binders. Subsequent studies could test these molecules in cell-based and in-vivo assays to gain understanding of the role of these isoforms in disease states. A promising approach for evaluating neuroplasticity would be to use organoids as a model for a mammalian brain.

MATERIALS AND METHODS

Docking and Design

The docking was done in Glide XP using Schrodinger Maestro (24). The software calculated the docking score on the basis of hydrogen bonding, electrostatic, hydrophobic and van der Waals forces. The docking score for compound 2 was -6.70 and compound 4 had a docking score of -6.96.

Synthesis of molecules

We synthesized compounds 3 and 4 in three steps, starting from commercially available 2,4-dichloro-1,8-naphthyridine (Figure 6). The first two reactions were aromatic nucleophilic substitution reactions (SNAr) (25). The first reaction used water in acidic conditions. The second used the appropriate amine with DIPEA in ethanol. The third reaction was a hydrogenation reaction using an H-Cube with 10% Pd/C as the catalyst to selectively reduce the pyridine ring to a piperidine ring in the presence of the pyridone (26). All ^{1}H and, for select compounds, ^{13}C NMR spectra were obtained on solution-state FT NMR instruments with proton operating frequency of 400 MHz and carbon operating frequency of 101 MHz. To avoid solubility challenges, all compounds were dissolved in deuterated DMSO.

4-(8-Aminooctylamino)-1H-1,8-naphthyridin-2-one (7)

Octane-1,8-diamine (264 mg, 1.83 mmol) and 4-chloro-1*H*-1,8-naphthyridin-2-one (114 mg, 0.63 mmol) were dissolved in ethanol (2.2 mL) and DIPEA (330 µL, 1.89 mmol, 1.0 eq). The vial was sealed and heated to 120 °C for 2.5 h in a microwave. The reaction was monitored by TLC (35% (2 M ammonia in methanol) in DCM), product Rf = 0.38. The reaction was concentrated *in vacuo*, and the residue was purified using automated column chromatography (gradient 0%-35% (2 M ammonia in methanol) in DCM). The Rf 0.38 fractions were combined and concentrated *in vacuo* to yield

https://doi.org/10.59720/24-033

4-(8-aminooctylamino)-1*H*-1,8-naphthyridin-2-one (181 mg, 0.326 mmol, 51.7% yield) as a cream solid. The crude ^{1}H (400 MHz, DMSO) NMR showed two impurities in the product: octane-1,8-diamine and 4-{8-[(2-oxo-1*H*-1,8-naphthyridin-4-yl)amino]octylamino}-1*H*-1,8-naphthyridin-2-one. Purity was estimated as 52% w/w.

8-[(2-Oxo-5,6,7,8-tetrahydro-1H-1,8-naphthyridin-4-yl) amino]octylammonium acetate (3)

4-(8-Aminooctylamino)-1*H*-1,8-naphthyridin-2-one (100 mg, 0.18 mmol) was dissolved in methanol (3 mL) and formic acid (3 mL) and pumped through the H-cube fitted with a 10% Pd/C cartridge at 40 °C, 50 bar, flow rate 0.5 mL/min. The solvent was concentrated *in vacuo* and the residue purified by prep-HPLC. Fractions were evaporated overnight in the GeneVac and 8-[(2-oxo-5,6,7,8-tetrahydro-1*H*-1,8-naphthyridin-4-yl)amino]octylammonium acetate (21.5 mg, 0.0610 mmol, 33.8% yield) was isolated as a salmon pink solid. ^{1}H NMR (400 MHz, DMSO) δ 5.47 – 5.38 (m, 2H), 4.56 (s, 1H), 3.13 – 3.07 (m, 2H), 2.96 (q, J = 6.6 Hz, 2H), 2.59 (t, J = 7.1 Hz, 2H), 2.16 (t, J = 6.4 Hz, 2H), 1.81 (s, 3H), 1.77 – 1.68 (m, 2H), 1.54 – 1.45 (m, 2H), 1. 45 – 1.35 (m, 2H), 1.33 – 1.23 (m, 8H).

4-(Tetrahydrofuran-3-ylmethylamino)-1H-1,8-naphthyridin-2-one (8)

4-Chloro-1*H*-1,8-naphthyridin-2-one (104 mg, 0.58 mmol) was added to a microwave vial, followed by ethanol (2.2 mL), DIPEA (301 uL, 1.73 mmol, 3 eq) and tetrahydrofuran-3-ylmethanamine (147 uL, 147 mmol, 2.5 eq). The vial was sealed and heated to 150 °C in the microwave for 4.5 h. The reaction was monitored by TLC (5% (2 M ammonia in methanol) in DCM), product Rf = 0.26. The reaction was concentrated *in vacuo*, and the residue was purified by automated column chromatography (0% to 10% (2 M ammonia in methanol) in DCM). The Rf 0.26 fractions were combined and concentrated *in vacuo* to yield 4-(tetrahydrofuran-3-ylmethylamino)-1H-1,8-naphthyridin-2-one (133mg, 0.4175mmol, 72.5% yield) as a cream solid. Crude 1H -NMR (400 MHz, DMSO) showed that the product contained tetrahydrofuran-3-ylmethanamine and purity was estimated as 77% w/w.

4-(Tetrahydrofuran-3-ylmethylamino)-5,6,7,8-tetrahydro-1H-1,8-naphthyridin-2-one (4)

4-(Tetrahydrofuran-3-ylmethylamino)-1*H*-1,8-naphthyridin-2-one (132 mg, 0.41 mmol) dissolved in methanol (4 mL) and formic acid (4 mL) was pumped through the H-Cube fitted with a 10% Pd/C cartridge at 40 °C, 20 bar, flow rate 0.5 mL/minute. The reaction was concentrated *in vacuo*, and 2 of the residue was purified by prep-HPLC. It was then evaporated overnight in the GeneVac to yield 4-(tetrahydrofuran-3-ylmethylamino)-5,6,7,8-tetrahydro-1*H*-1,8-naphthyridin-2-one (17.9 mg, 0.0718 mmol, 69% yield) as a purple solid. 1H NMR (400 MHz, DMSO) δ 9.65 (br s, 1H), 5.59 (t, J = 5.6 Hz, 1H), 5.34 – 5.29 (m, 1H), 4.61 (s, 1H), 3.73 (td, J = 8.0, 5.7 Hz, 1H), 3.64 (dd, J = 8.6, 6.9 Hz, 1H), 3.63 – 3.56 (m, 1H), 3.45 (dd, J = 8.5, 4.9 Hz, 1H), 3.14 – 3.09 (m, 2H), 2.94 (dd, J = 7.3, 5.6 Hz, 2H), 2.55 – 2.42 (m, 1H), 2.17 (t, J = 6.4 Hz, 2H), 1.99 – 1.86 (m, 1H), 1.73 (p, J = 6.2 Hz, 2H), 1.61 – 1.50 (m, 1H). ^{13}C NMR (101 MHz, DMSO) δ 162.2, 156.7, 146.2, 82.0, 81.0, 71.1, 67.2, 45.6, 38.2, 30.0, 21.7, 19.5.

Nucleotide exchange assay

Test compounds were dissolved in DMSO to a 50 mM concentration then diluted to 500 µM with assay buffer, the composition of which is described below. This 500 µM stock solution was used to make 10 2-in-1 serial dilutions for a dose response curve. 5 µL of the compound solution was dispensed into each vial. 10 µL of an assay buffer consisting of 20 mM Tris pH 7.5, 50 mM NaCl, 1 mM MgCl2, 100 µg/mL BSA, and 1mM DTT was dispensed into each well except for the control GppNHp wells. 10 µL of 400 µM GppNHp (Jena BioScience) in 20 mM tris pH 7.5, 50 mM NaCl was added to each positive control well. The enzymes were mixed to a final concentration of 4 µM RAC1 and 0.1 µM kalirin in the assay buffer, and 5 µL of this mix was dispensed to every well. The assay was incubated at 20 °C for 2 h. 5 µL of 2 µM BODIPYL GTP (ThermoFisher Scientific) in assay buffer was dispensed to each well. The plate was then shaken for 10 seconds, and fluorescence intensity signal was measured every 30 seconds for 5 min using the PherastarFSX (BMG Labtech, FI 485/520, Gain 300). The initial enzyme rate was calculated and normalized to the GppNHp control.

ACKNOWLEDGMENTS

This work was funded by a grant (ARUK-2021DDI-X) from Alzheimer's Research UK.

Received: January 15, 2024
Accepted: July 13, 2024
Published: November 04, 2024

REFERENCES

1. Mould, Arne W., et al. "Kalirin as a Novel Treatment Target for Cognitive Dysfunction in Schizophrenia." *CNS Drugs*, vol. 36, no. 1, 2022, pp. 1-16. https://doi.org/10.1007/s40263-021-00884-z.
2. Owen, Michael J., et al. "Schizophrenia." *The Lancet*, vol. 388, no. 10039, 2016, pp. 86-97. https://doi.org/10.1016/S0140-6736(15)01121-6.
3. Glantz, Leisa A., and Lewis, David A. "Decreased Dendritic Spine Density on Prefrontal Cortical Pyramidal Neurons in Schizophrenia." *Archives of General Psychiatry*, vol. 57, no. 1, 2000, pp. 65-73. https://doi.org/10.1001/archpsyc.57.1.65.
4. Black, James E., et al. "Pathology of Layer V Pyramidal Neurons in the Prefrontal Cortex of Patients with Schizophrenia." *American Journal of Psychiatry*, vol. 161, no. 4, 2002, pp. 742-744. https://doi.org/10.1176/appi.ajp.161.4.742.
5. Onwordi, Ellis C., et al. "Synaptic Density Marker SV2A is Reduced in Schizophrenia Patients and Unaffected by Antipsychotics in Rats". *Nature Communications*, vol. 11, no. 1, 2020. https://doi.org/10.1038/s41467-019-14122-0.
6. Law, Amanda, et al. "Reduced Spinophilin But Not Microtubule-Associated Protein 2 Expression in the Hippocampal Formation in Schizophrenia and Mood Disorders: Molecular Evidence for a Pathology of Dendritic Spines." *American Journal of Psychiatry,* vol. 161, no. 10, 2004, pp. 1848–1855. https://doi.org/10.1176/ajp.161.10.1848.
7. Ripke, Stephan, et al. "Biological Insights From 108 Schizophrenia-Associated Genetic Loci." *Nature*, vol.

https://doi.org/10.59720/24-033

511, no. 7510, 2014, pp. 421-427. https://doi.org/10.1038/nature13595.
8. Trubetskoy, Vassily, et al. "Mapping Genomic Loci Implicates Genes and Synaptic Biology in Schizophrenia." *Nature,* vol. 604, 2022, pp. 502-508. https://doi.org/10.1038/s41586-022-04434-5.
9. Paskus, Jeremiah D., et al. "Kalirin and Trio: RhoGEFs in Synaptic Transmission, Plasticity, and Complex Brain Disorders." *Trends in Neurosciences,* vol. 43, no. 7, 2020, pp. 505–518. https://doi.org/10.1016/j.tins.2020.05.002.
10. Christine Remmers, Robert A. Sweet,and Peter Penzes, Abnormal Kalirin Signaling in Neuropsychiatric Disorders, Brain Res Bull. 2014 Apr; 0: 29–38. https://doi.org/10.1016/j.brainresbull.2013.12.006.6
11. Kushima, Itaru, et al. "" Resequencing and Association Analysis of the KALRN and EPHB1 Genes And Their Contribution to Schizophrenia Susceptibility." *Schizophrenia Bulletin*, Volume 38, no. 3, 2012, pp. 552–560. https://doi.org/10.1093/schbul/sbq118Hlushchenko.
12. , Iryna, et al. "Dendritic Spine Actin Dynamics in Neuronal Maturation and Synaptic Plasticity." *Cytoskeleton*, vol. 73, no. 9, 2016, pp. 435-441. https://doi.org/10.1002/cm.21280.
13. Luo, Liqun. "Actin Cytoskeleton Regulation in Neuronal Morphogenesis and Structural Plasticity." *Annual Review of Cell and Developmental Biology*, vol. 18, no. 1, 2002, pp. 601–635. https://doi.org/10.1146/annurev.cellbio.18.031802.150501.
14. Mosaddeghzadeh, Niloufar, and Ahmadian, Mohammad R. "The RHO Family GTPases: Mechanisms of Regulation and Signaling." *Cells*, vol. 10, no. 7:1831, 2021. https://doi.org/10.3390/cells10071831.
15. Haditsch, Ursula, et al. "A Central Role for the Small GTPase RAC1 in Hippocampal Plasticity and Spatial Learning and Memory." *Molecular and Cellular Neuroscience*, vol. 41, no. 4, 2009, pp. 409–419. https://doi.org/10.1016/j.mcn.2009.04.005.
16. Johnson, Richard C., et al. "Isoforms of Kalirin, a Neuronal Dbl Family Member, Generated Through Use of Different 5'- and 3'-Ends Along With An Internal Translational Initiation Site." *Journal of Biological Chemistry*, vol. 275, no. 25, 2000, pp. 19324-19333. https://doi.org/10.1074/jbc.m000676200.
17. McPherson, Clifton E., et al. "Genomic Organization and Differential Expression of Kalirin Isoforms." *Gene*, vol. 284, no. 1-2, 2002, pp. 41–51. https://doi.org/10.1016/s0378-1119(02)00386-4.
18. Mains, Richard E., et al. "Kalrn promoter usage and isoform expression respond to chronic cocaine exposure." *BMC Neuroscience*, vol. 12, no. 1, 2011, pp. 12-20. https://doi.org/10.1186/1471-2202-12-20.
19. Miller, Megan B., et al. "An N-terminal Amphipathic Helix Binds Phosphoinositides and Enhances Kalirin Sec14 Domain-mediated Membrane Interactions." *Journal of Biological Chemistry*, vol. 90, no. 21, 2015, pp. 13541-13555. https://doi.org/10.1074/jbc.m115.636746.
20. Kushima, Itaru, et al. "Resequencing and Association Analysis of the KALRN and 15 EPHB1 Genes and Their Contribution to Schizophrenia Susceptibility." *Schizophrenia Bulletin*, vol. 38, no. 3, 2012, pp. 552–560. https://doi.org/10.1093/schbul/sbq118.
21. Gulsuner, Suleyman, et al. "Genetics of Schizophrenia in the South African Xhosa." *Science*, vol. 367, no. 6477, 2020, pp. 569–573. https://doi.org/10.1126/science.aay8833.
22. Russell, Theron A., et al. "A Sequence Variant in Human KALRN Impairs Protein Function and Coincides with Reduced Cortical Thickness." *Nature Communications*, vol. 5, no. 1:4858, 2014. https://doi.org/10.1038/ncomms5858.
23. Gray, Janine L., et al. "Human Kalirin/RAC1 GEF/GTPase Complex." [Data set]. *Zenodo*, 2019. https://doi.org/10.5281/zenodo.3266933.
24. Yang, Ying., et al. "Efficient exploration of chemical space with docking and deep learning." *Journal of Chemical Theory and Computation,* vol. 17, no. 1, 2021, pp. 7106-7119. https://doi.org/10.1021/acs.jctc.1c00810.
25. Terrier, François. *Modern Nucleophilic Aromatic Substitution*. John Wiley & Sons, 2013.
26. Zhou, Yong-Gui. "Asymmetric Hydrogenation of Heteroaromatic Compounds." *Accounts of Chemical Research*, vol. 40, no. 12, 2007, pp. 1357-1366. https://doi.org/10.1021/ar700094b.